Image Quality Assessment with a Gabor Pyramid Model of the Human Visual System

Christopher C. Taylor[†], Zygmunt Pizlo[‡], Jan P. Allebach[†], and Charles A. Bouman[†]

[†]Electronic Imaging Systems Laboratory
Purdue University, School of Electrical and Computer Engineering
West Lafayette, IN 47907-1285
{taylor,allebach,bouman}@ecn.purdue.edu

[‡]Purdue University, Department of Psychological Sciences
West Lafayette, IN 47907
pizlo@psych.purdue.edu

ABSTRACT

Reliable image quality assessments are necessary for evaluating digital imaging methods (halftoning techniques) and products (printers, displays). Typically the quality of the imaging method or product is evaluated by comparing the fidelity of an image before and after processing by the imaging method or product. It is well established that simple approaches like mean squared error do not provide meaningful measures of image fidelity. A number of image fidelity metrics have been developed whose goal was to predict the amount of differences that would be visible to a human observer. In this paper we outline a new model of the human visual system (HVS) and show how this model can be used in image quality assessment. Our model departs from previous approaches in three ways: 1) We use a physiologically and psychophysically plausible Gabor pyramid to model a receptive field decomposition; 2) We use psychophysical experiments that directly assess the percept we wish to model; and 3) We model discrimination performance by using discrimination thresholds instead of detection thresholds. The first psychophysical experiment tested the visual system's sensitivity as a function of spatial frequency, orientation, and average luminance. The second experiment tested the relation between contrast detection and contrast discrimination.

Keywords: Image fidelity, Image quality, Gabor, human visual system, detection, discrimination

1 INTRODUCTION

Before we describe our model, we briefly review a number of contributions of researchers working in the areas of image processing and image understanding. Each of these two areas has produced models of the HVS that were intended to meet application specific criteria. The emphasis of image processing research was on descriptive models, i.e. models that are supposed to produce evaluations of image quality similar to those of a human observer, regardless of whether the models involved computations analogous to perceptual mechanisms. A potential problem with purely descriptive models is that they may not generalize to cases that differ from those used to formulate these models. Such generalizations are more likely in the case of explanatory models, i.e. models that are supposed to involve computations analogous to perceptual and physiological mechanisms. Explanatory models of the HVS are being formulated within the area of image understanding, which is concerned with deriving perceptual interpretations from images.

Image quality measures have been particularly intriguing for those studying lossy image compression.[1–5] The goal of image compression is to discard as much information as possible while maintaining a certain level of image quality. Typically this is done by processing images in a perceptual space. By the nature of the
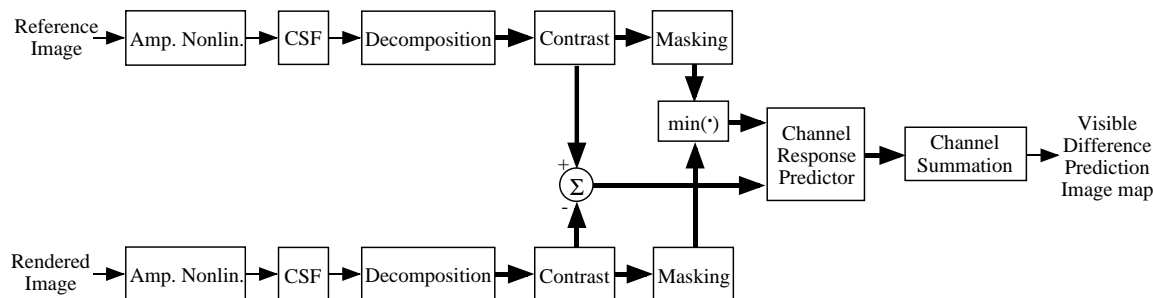
Figure 1: Block diagram of Daly's visible differences predictor.

problem, all such algorithms are constrained by the necessity that the transform into the perceptual space be complete (invertible). Even in areas unrelated to image compression, this invertibility constraint continues to be enforced.[6–11] While such a constraint may be attractive in allowing a more diverse set of applications for a visual model, it comes at a cost of less physiologically and psychophysically plausible models of the HVS. Our emphasis on modeling percept leads to three modifications of prior approaches. These modifications consist of 1) using a physiologically and psychophysically plausible Gabor pyramid to model a receptive field decomposition, 2) using psychophysical experiments that directly assess the percept we wish to model, and 3) modeling discrimination performance by using discrimination thresholds instead of detection thresholds.

A number of models incorporating some type of frequency selective channels have been proposed for image fidelity assessment.[6–11] These models have made great progress towards attaining meaningful image fidelity assessments. They go far beyond simple mean-squared error, which is well-known to be unsatisfactory. Our work has been heavily influenced by these models and attempts to build on them. In order to motivate our approach, we begin by considering some of the characteristics of these models. Figure 1 contains a block diagram for one representative model.[6] The two images being compared are processed by an amplitude nonlinearity and a contrast sensitivity function (CSF). They are then decomposed into visual channels. A local contrast calculation is done for each channel, and a masking computation determines a threshold elevation. The difference of the two contrast images is compared to the elevated detection threshold to determine the visibility of differences between the two channel images. In the final stage, the visibility predictions in each channel are then combined to provide a measure of image fidelity. In this model, a variety of psychophysical data is used. The CSF is based on a set of psychophysical experiments not directly related to the set of experiments for which the threshold elevation curves for masking are based. Likewise, the amplitude nonlinearity, decomposition, and contrast calculations are founded on still others' experiments. Frequently the task performed in the experiment used to obtain model parameters is not directly related to the function of the corresponding portion of the model. For example, psychophysical experiments that determine the CSF lead to the relation between contrast and percept, i.e. the probability of seeing a sine grating at a particular frequency and contrast. However, the output of the CSF in Fig. 1 is not probability. This means that this portion of the model is not a model of percept. Other models share these characteristics. We have endeavored to take a more integrated approach with the goal of having our model more closely match the psychophysical experiments upon which it is based.

Over the past 35 years, psychophysical and physiological experiments have been performed to examine the response of the visual system to patterns that vary in spatial frequency or orientation. In the process, there were those who viewed the function of the early visual system as spatially localized feature detection[12] and those who viewed it as a Fourier-like spatial frequency decomposition.[13,14] In the early 1980's the two approaches seemed to merge as Marčelja[15] directed attention to a paper by Gabor[16] that formulated an uncertainty relation for information. For 1D signals, Gabor showed that a lower bound exists on the product of the ability to resolve a signal in frequency and the ability to resolve a signal in time. Furthermore, Gabor described a family of signals that obtain a lower limit of joint uncertainty in time and frequency. Daugman[17] has extended Gabor's work to two dimensions to show that Gabor patches minimize the uncertainty relations for the joint 2D-spatial—2D-spectral space. A number of physiological studies on cats and primates have confirmed the hypothesis that mammalian visual systems contain neurons whose receptive fields closely resemble Gabor patches.[18–22]

Since Gabor decompositions are not orthogonal, prior image quality assessment methods have preferred to decompose the image by sectioning the frequency domain into a number of pie pieces. On the other hand, Gabor decompositions have been used to address a number of image understanding problems. Many texture segmentation and classification techniques have relied on Gabor decompositions.[23-29] In addition, Cannon[30] constructed a Gabor based model that successfully predicts perceived image sharpness of spatially filtered real world scenes. Because of the physiological and psychophysical plausibility of a Gabor decomposition, our model involves a Gabor pyramid. Our psychophysical experiments determine the parameters of the model. The first experiment tested the visual system's sensitivity to Gabor patches as a function of spatial frequency, orientation, and average luminance.

Our second psychophysical experiment compared the relation between detection and discrimination thresholds. The motivation for this second experiment is as follows. Prior image fidelity measures implicitly assume that contrast detection and contrast discrimination are equivalent.[6-9,11] In contrast detection experiments the subject is asked whether or not the stimulus is visible. In contrast discrimination experiments the subject is asked to discriminate between two stimuli. When the subject is asked to discriminate between a stimulus and no stimulus, the discrimination task may seem to be equivalent to the detection task. It is tempting to assume that detection and discrimination experiments produce the same thresholds. For example, one could conclude that for a particular stimulus with a detection threshold of 4% contrast, the same subject would be able to discriminate between the presence or absence of the same stimulus with 4% contrast with the same probability as in the detection experiment. One may even conclude that the discriminability between stimuli of 25% and 29% contrast or between stimuli of 80% and 84% contrast would be identical. Regardless of how reasonable these conclusions may or may not be, this is precisely what prior models for image fidelity assessment have done. This fact is illustrated in Fig. 1. The difference of the two contrast images is computed in this model just prior to the channel response predictor. At this point, the information about the contrast in the original images is lost, and the results of contrast detection experiments are used to determine the visibility thresholds. A number of studies[31-33] under slightly different conditions have shown that this assumption is not valid. Our second psychophysical experiment further explored the relationship between contrast detection and contrast discrimination using Gabor patches as stimuli.

2   MODEL

Our goal is to develop a model of the HVS that is both physiologically plausible and consistent with psychophysical data. In doing so, we derive a multiresolution (pyramid) approach for modeling receptive fields that are localized in both the spatial and spatial frequency domains.

Close examination of the processing of the HVS indicates that it operates using pyramid-style parallelism. Rapid discrimination of objects in images is one example. It is possible to recognize objects in complex images in a fraction of a second. Such ability would not be possible without a highly parallel visual system. A pyramid structure provides a reasonable explanation for this, as well as many other perceptual phenomena.[34-37] Equipped with these findings and those in the previous section, we describe a model of image fidelity based on a Gabor pyramid.

Our model accepts two grayscale images as inputs and generates a probability map as output. The probability map is a grayscale image that indicates the probability of a human observer locally detecting a difference between the two input images at each pixel. A block diagram of our model is shown in Fig. 2. The model departs significantly from prior approaches in that the Gabor pyramid decomposition is matched with the psychometric functions used to predict the visibility of differences between the two input images.

A multiresolution decomposition is performed on each image to generate a number of channels, each containing the response of an ensemble of visual receptors. The receptors are modeled by Gabor functions of varying frequency and orientation whose features are similar to the receptive fields of the neurons in the primary visual cortex. The characteristics of the Gabor functions used in our model follow those of Lee[38] and are motivated by the work of many others.[39-43,17,18,21,14,22,19] The decomposition used in our model is based on the following considerations:

- Gabor patches have optimal localization in both the spatial and spectral domains.[16,17]
- Pairs of simple cells exhibit constant quadrature phase.[40,22,44]
- Receptive fields are elliptical with an aspect ratio of 2:1 and modulation along the short axis of the ellipse.[19,17]
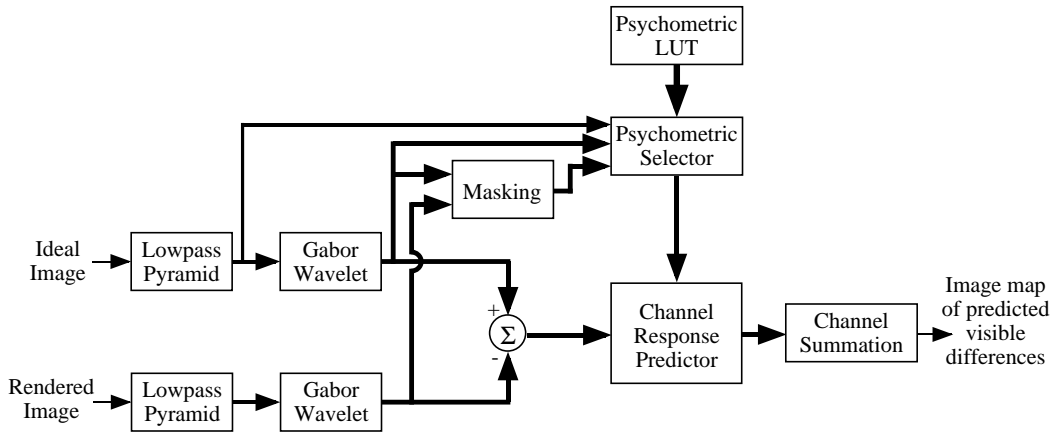
Figure 2: Block diagram of our HVS model.
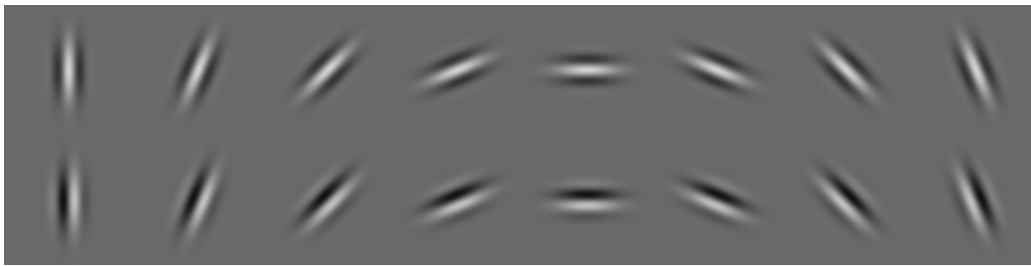
Figure 3: The set of Gabor filters. The top row contains the even symmetric components and the bottom row contains the odd symmetric components.

- Receptive fields have a spatial frequency bandwidth predominately located around 1.5 octaves.[19,41,45]
- Receptive fields have a orientation bandwidth around 20°.[41]
- Receptive fields are shape invariant.[46]

The Gabor patches for one resolution level of the pyramid are shown in Fig. 3.

The multiresolution pyramid is built by lowpass filtering and decimating the original image as shown in Fig. 4. We call each output image the *base image* for a particular pyramid level. Figure 5 outlines the Gabor decomposition for one level of the pyramid. The base image for each pyramid level is convolved with even and odd symmetric Gabor wavelets at eight orientations. The square root of the sum of the squares of the resulting even-odd image pairs describes the response of an ensemble of neurons tuned to a particular spatial frequency and orientation. We call these images the *channel images* as they represent different channels of the visual system.

Due to the nature of Gabor patches, the resulting output from the decomposition is already a measure of contrast, and hence, no additional contrast calculation is needed. At this point, we have not addressed the issue of masking. The masking component in the Fig. 2 represents future work.

The Psychometric Look Up Table (LUT) consists of a family of psychometric functions that have been empirically determined by psychophysical experiments described below. The Psychometric Selector selects the appropriate psychometric function from the family of psychometric functions in the Psychometric LUT. A higher pyramid level base image determines the adaptation level, and the channel image determines the frequency, orientation, and reference contrast levels used to select the appropriate psychometric function from the LUT.

The difference between the contrast images for each channel is then applied to the appropriate psychometric function to produce a separate probability map for each channel. For example, the psychometric function plotted in Fig. 6 would yield a visibility prediction of 0.8 for a contrast difference of 5%. All of the probability maps from the different channels are combined using probability summation to generate the final probability map.
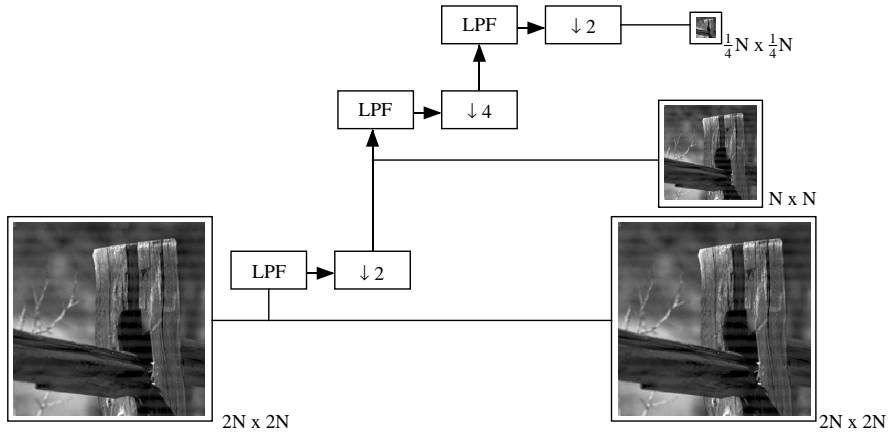
Figure 4: Lowpass pyramid decomposition.
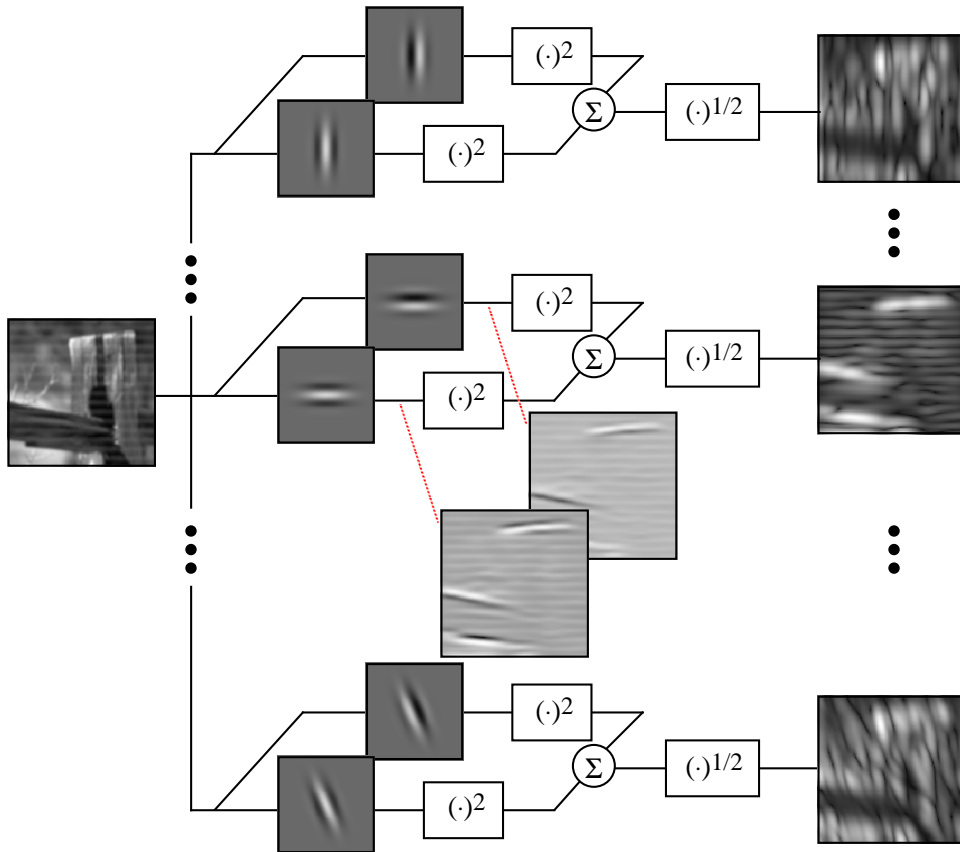
Figure 5: Gabor channel decomposition.
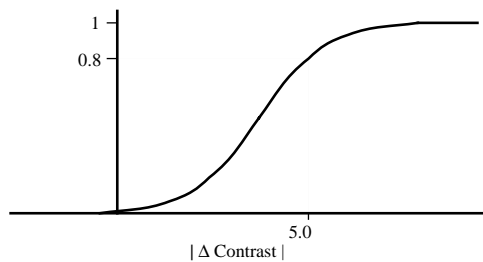
Figure 6: Example psychometric function.

3 DETECTION EXPERIMENT

The psychometric functions in our model represent the contrast sensitivity of the HVS as a function of frequency, orientation, and luminance. Psychophysical experiments to measure contrast sensitivity are not new. A number of experiments have measured sensitivity to sine waves and/or square waves at different luminance levels.[47–50] Losada, *et al.*[51] measured sensitivity to sine waves for different frequencies and orientations at three luminance levels. However, we are interested in the visual system's sensitivity to Gabor patches. Peli, *et al.*[52] reported such an experiment, but the experiment was limited to Gabor patches that deviate in shape from those in our model. Furthermore, only two orientations (0 and 90°) and only one luminance level were tested. Therefore, we designed a psychophysical experiment to measure contrast sensitivity as a function of frequency, orientation, and luminance of Gabor patches.

3.1 Apparatus

Gabor patches were generated on a calibrated 24-bit color monitor with a peak luminance of 70 cd/m^2 and a gamma of 2.25. The monitor displays square pixels at a resolution of 100 pixels per inch on a 1024×1280 pixel screen. All stimuli were gamma corrected and displayed in a dark room. The presentation time was controlled by a Hewlett-Packard workstation. A chin rest was used to stabilize the subject's head at the appropriate viewing distance. For all but the two lowest frequencies, a viewing distance of 2.4 m was used.[*] For the two lowest frequency sessions, the viewing distance was reduced to one meter. Stimuli were always displayed on the monitor with an average luminance of 35 cd/m^2. Neutral density filters were used to obtain the correct average luminance.

3.2 Subjects

Two of the authors (CCT, JPA) served as subjects in the experiment. CCT was a slight myope and JPA was a myope. Both subjects wore their normal correcting glasses. The subjects viewed the stimuli with the natural pupil of their dominant eye.

3.3 Stimulus

In our experiment we deviate from the standard sine wave in favor of a psychophysically and physiologically motivated Gabor patch. The Gabor patch models the receptive fields of the HVS and is characterized as follows:

$$R(x,y;f_0,\theta) = L_{ave}\left(1 + Ce^{\frac{-1}{\sqrt{\pi\alpha\sigma^2}}((\alpha^2(x\cos\theta+y\sin\theta)^2+(y\cos\theta-x\sin\theta)^2)}e^{if_0(x\cos\theta+y\sin\theta)}\right)$$

where x and y are the horizontal and vertical distance from center, f_0 and θ are the frequency and orientation of the sinusoidal grating, α and σ are the aspect ratio and standard deviation for the Gaussian envelope, C is the contrast of the Gabor patch, and L_{ave} is the average luminance of the Gabor patch.

A few additional considerations arise with this change in stimulus. We define contrast as $C = L_{peak}/L_{ave}$. This definition is equivalent to the contrast definition proposed by King-Smith and Kulikowski[53] and the nominal contrast defined by Watson.[10] In the case of a sine wave this definition of contrast is equivalent to the popular Michelson contrast, since $L_{peak} = L_{max} - L_{ave} = L_{ave} - L_{min}$, i.e.

$$C = \frac{L_{peak}}{L_{ave}} = \frac{L_{peak} + L_{peak}}{2L_{ave}} = \frac{L_{max} - L_{min}}{L_{max} + L_{min}}.$$

However, this is not the case with the Gabor patch. The Gabor patch is a sine wave in a Gaussian envelope. The Gaussian envelope attenuates the trough of the sine wave, effectively increasing L_{min} so that the above equation no longer holds. In addition, the attenuating effect of the Gaussian envelope causes low contrast Gabor patches to appear smaller than high contrast Gabor patches. For small changes in contrast, the perceived change in size is minimal.[54] Consequently, the contrast remains the salient feature in detecting and discriminating Gabor patches.

---

[*]The size of the room required the use of a front surface reflecting mirror to achieve a viewing distance of 2.4 m.
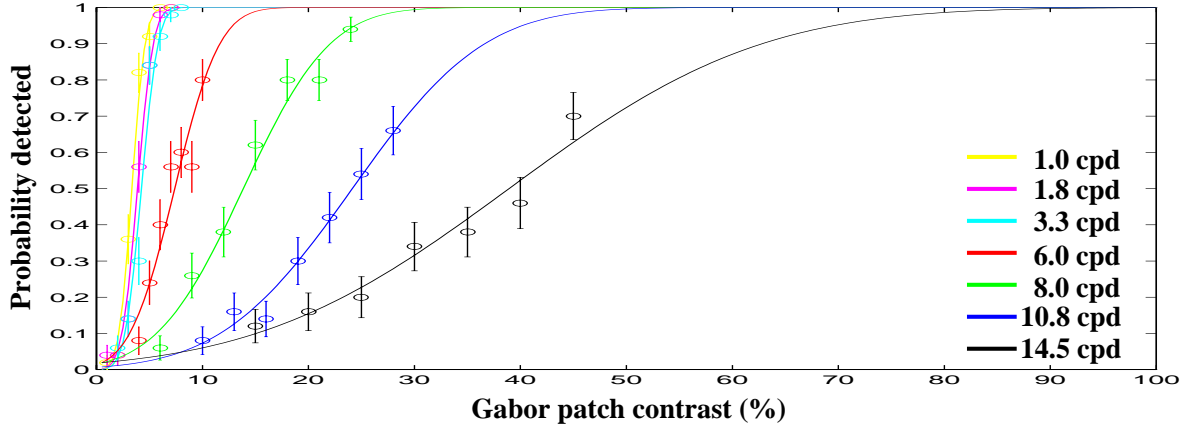
Figure 7: Psychometric functions for vertically oriented Gabor patches with an average luminance of 4.4 cd/m².

3.4 Procedure

The stimulus was characterized by average luminance, contrast, frequency, and orientation. In a single session, all but contrast were held constant. The target consisted of a Gabor patch in the center of a uniform gray image with luminance L_{ave}. The method of constant stimuli was used. Within a session eight levels of contrast were presented. One contrast level was set at 0%. Trials with 0% contrast served as "catch" trials. Fifty trials of each stimulus were presented in random order for a total of 400 trials per session.

A fixation cross was displayed before and after each trial. Each trial was initiated by pressing the middle mouse button whereupon a 50 ms average luminance uniform field was presented followed by a 100 ms presentation of the trial stimulus. The subject then pressed the left mouse button if he saw the stimulus or the right mouse button if he did not see the stimulus. The subject was instructed to adopt a response criterion such that the proportion of errors on the catch trials was low but above zero. Auditory feedback was provided after each catch trial presentation.

The result of each session was a psychometric function indicating the probability of the subject detecting the given Gabor patch at various contrast levels. This data was analyzed with SAS version 6.11 using probit analysis[55] to obtain contrast detection thresholds.

Both subjects completed sessions for eight orientations (0, 22.5, 45, 67.5, 90, 112.5, 135, and 157.5°) and three average luminance levels (0.5, 4.4, and 35 cd/m²) using Gabor patches of 6 cycles/degree (c/deg). In addition, subject CCT completed sessions for ten spatial frequencies (1, 1.8, 3.3, 6, 8, 10.8 14.5, 19.4, 26.1, and 35 c/deg at the above average luminances using vertically oriented Gabor patches. Subject CCT also produced psychometric functions for 6 c/deg vertically oriented Gabor patches at eight different luminance levels (0.5, 1.1, 2.2, 4.4, 8.8, 17.5, and 35 cd/m²).

3.5 Results

The obtained psychometric functions for subject CCT with vertically oriented Gabor patches with an average luminance of 4.4 cd/m² and varying spatial frequencies are plotted in Fig. 7. The smooth curves are cumulative Gaussian functions fit to the data via probit analysis. The psychometric functions reveal the probability that the subject detected the Gabor patch for various contrasts. The psychometric function for the 1 c/deg Gabor patch has the steepest slope. As spatial frequency increases the psychometric functions are shallower, indicating the subject's reduced sensitivity (1/threshold) to Gabor patches at those spatial frequencies. The three curves in Fig. 8 represent the visual sensitivity for the three luminances measured as a function of spatial frequency.

Figure 9 contains the thresholds obtained for 6 c/deg Gabor patches of various orientations for both subjects. In each plot, the three curves represent average luminance levels of 0.5, 4.4, and 35 cd/m². The thresholds for subject CCT with a vertically oriented, 6 c/deg Gabor patch are plotted in Fig. 10 as a function of average luminance.
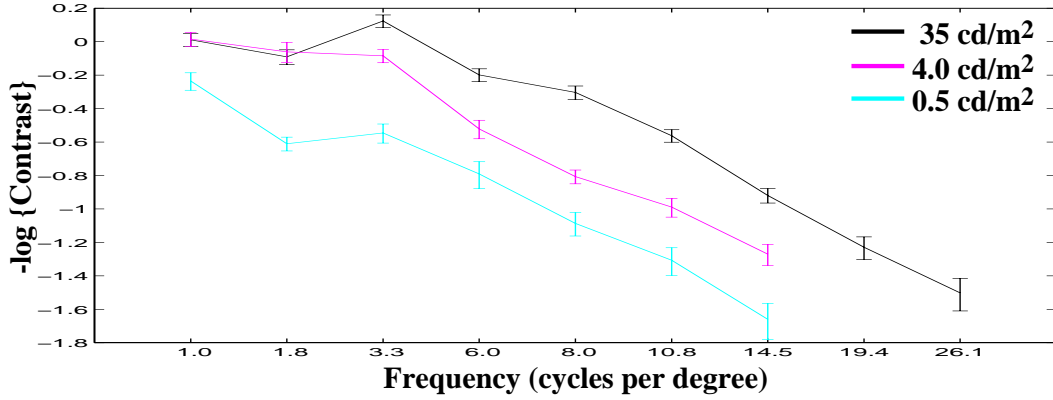
Figure 8: Sensitivity curves for vertically oriented Gabor patches at various average luminance levels.
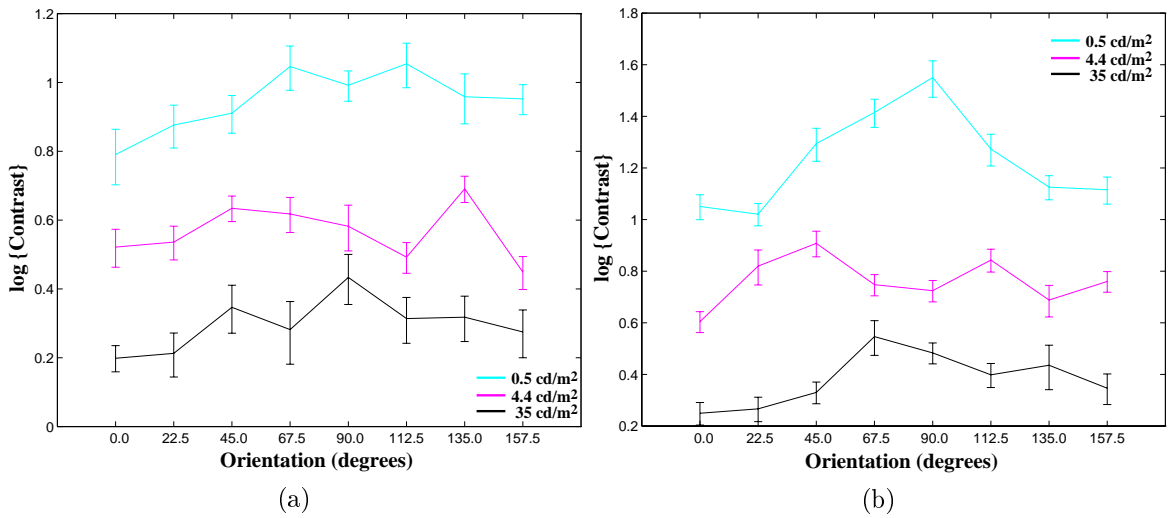
Figure 9: Detection thresholds for (a) CCT and (b) JPA for 6 c/deg Gabor patches at various orientations.

3.6 Discussion

The sensitivity data in Fig. 8 indicate a lowpass nature for the sensitivity of the HVS to Gabor patches. The data match that of two similar studies[51,47] for frequencies above 3 c/deg. Losada et $al.$ measured the contrast sensitivity to sine wave gratings with average luminance levels of 0.05, 0.5, and 20 cd/m^2. Banks et $al.$[47] measured the contrast sensitivity to cosine gratings damped horizontally and vertically by a half-cosine wave adjusted to encompass 7.5 cycles of the cosine. They considered spatial frequencies from 5 to 40 c/deg and average luminance levels of 3.4, 34, and 340 cd/m^2. Losada et $al.$ found a decrease in sensitivity to sine wave gratings below 3 c/deg. We did not observe this decrease in sensitivity at low frequencies. Instead, our curves exhibited a lowpass shape consistent with those reported by Peli et $al.$ Figure 9 shows that the contrast detection depends on the orientation of the stimulus. The general shape of the curves is consistent with those obtained by others.[51]

It can be observed in Fig. 10 that the contrast thresholds decrease as the average luminance increases until 9 cd/m^2. The luminance levels below this value represent a range in which Weber's law does not hold. However, for luminance levels above 9 cd/m^2, the reduction in contrast thresholds lessens implying an approximation of Weber's law for this range of luminance levels. Banks et $al.$ reported that contrast sensitivity was higher at luminance levels of 340 cd/m^2 than at 34 cd/m^2 but that the decrease in threshold was not as large as from 3.4 to 34 cd/m^2. Due to peak luminance limitations with our display device, we were unable to investigate contrast sensitivity for luminance greater than 35 cd/m^2.
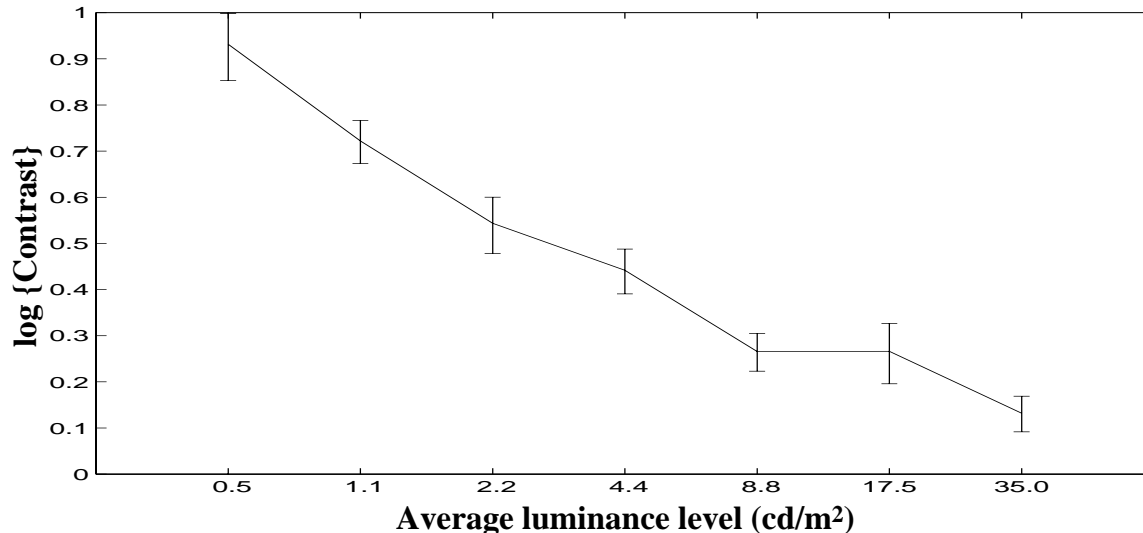
Figure 10: Thresholds for 6 c/deg vertically oriented Gabor patches at various luminance levels.

4   DISCRIMINATION EXPERIMENT

Image fidelity assessments are based on the task of discrimination, i.e. the task of perceiving differences between two stimuli. However, typical image fidelity metrics use models based on detection thresholds, i.e. thresholds based on the ability to perceive a single stimulus. In this experiment we explore the relationship between detection and discrimination tasks. We employed the same apparatus as in the detection experiment and used a viewing distance of 2.4 m.

4.1   Subjects

Three subjects including two of the authors (CCT, ZP) served in the experiment. ZP and TF were myopes. The subjects wore their normal correcting glasses and viewed the stimuli binocularly with natural pupils.

4.2   Procedure

The stimulus consisted of two vertically oriented, 6 c/deg Gabor patches with the same characteristics as those in the previous experiment. The reference patch had a fixed contrast while the test patch varied in contrast. Within a session the test patch consisted of eight contrast levels slightly above reference contrast. A fixation cross remained at the center of a uniform gray image with luminance L_{ave} throughout each session. In each trial the two Gabor patches were presented 1° to either side of the fixation cross. The presentation time for each trial was 100 ms. Each test patch was presented 100 times for a total of 800 trials per session.[†] The test patches were presented in random order, and the side of presentation for the test and reference patches was randomized with each trial.

The subject was asked to indicate which patch (left or right) had higher contrast. Auditory feedback was provided whenever the subject responded incorrectly. The psychometric functions were analyzed using probit analysis to obtain contrast discrimination thresholds. All subjects completed sessions for four reference contrast levels (0, 25, 50, and 75%) at an average luminance level of 35 cd/m^2. In addition, subject CCT completed sessions for reference contrast levels of 3 and 9% at 35 cd/m^2 and reference contrast levels of 0, 25, 50, and 75% for an average luminance level of 4.4 cd/m^2.

[†]Some of the sessions involved 50 presentations of each test patch for a total of 400 trials per session.
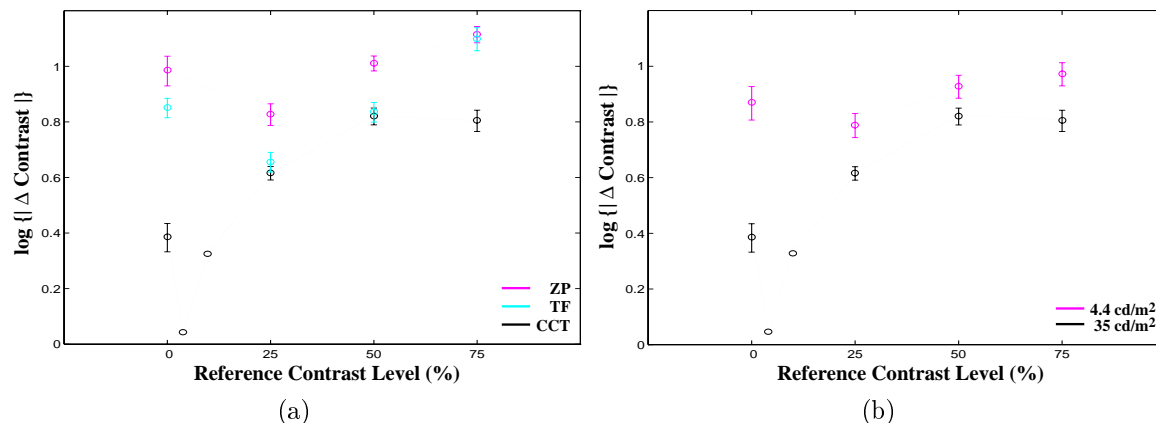
Figure 11: Thresholds for Discrimination of 6 c/deg vertically oriented Gabor patches for (a) three subjects at 35 cd m^{-2} average luminance and (b) subject CCT at two average luminance levels.

4.3 Results

The results from this experiment are presented in Fig. 11. Figure 11a contains curves of the discrimination threshold as a function of reference contrast for all three subjects using Gabor patches at an average luminance level of 35 cd/m^2. Figure 11b compares the thresholds for subject CCT at two average luminance levels.

4.4 Discussion

It is clear from Fig. 11 that discrimination and detection tasks are not equivalent. If they were, then all of the curves would be horizontal lines. This observation is consistent with the results of previous experiments. Typically these experiments have presented two sine wave gratings in temporal succession and asked the subject to indicate the grating of higher contrast.[31-33] The case of 0% reference contrast is analogous to the detection task. We see that as the reference contrast increases, the discrimination threshold decreases and then increases. The facilitation effect observed for low reference contrasts has been reported in previous studies; however, with the exception of the 35 cd/m^2 case for subject CCT, the facilitation effects continue well beyond the reference contrasts reported previously. In addition, it should be noted that only the curve for CCT with average luminance of 35 cd/m^2 contains data points for reference contrasts of 3 and 9%. We would expect a similar dramatic facilitation effect to be evident had this data been collected for the other curves.

Finally, it is interesting to note that a higher variability exists in the detection thresholds than the discrimination thresholds. This is true both among various subjects (Fig. 11a) and among different average luminance levels for the same subject (Fig. 11b). This observation suggests that two independent mechanisms may be responsible for the detection and discrimination tasks. To that end, a model that is based on discrimination thresholds appears to be more psychophysically plausible.

ACKNOWLEDGMENT

5   REFERENCES

[1] N. S. Jayant, J. D. Johnston, and R. J. Safranek, "Signal compression based on models of human perception," *Proc. of the IEEE*, vol. 81, no. 10, pp. 1385 – 1422, 1993.

[2] A. B. Watson and A. J. Ahumada, Jr., "A hexagonal orthogonal-oriented pyramid as a model of image representation in visual cortex," *IEEE Trans. Biomed. Eng.*, vol. 36, no. 1, pp. 97 – 106, 1989.

[3] A. B. Watson, "Efficiency of an image code based on human vision," *J. Opt. Soc. Am. A*, vol. 4, no. 12, pp. 2401

– 2417, 1987.

[4] J. A. Solomon, A. B. Watson, and A. Ahumada, "Visibility of DCT basis functions: effects of contrast masking," *Proc. of Data Compression Conf.*, Mar 1994, Snowbird, UT, USA, pp. 361 – 370.

[5] A. B. Watson, "Perceptual optimization of DCT color quantization matrices," *Proc. of IEEE Int'l Conf. on Image Proc.*, vol. 1, Nov. 1994, Austin, TX, USA, pp. 100 – 104.

[6] S. Daly, "The visible differences predictor: An algorithm for the assessment of image fidelity," in *Digital Images and Human Vision* (A. B. Watson, ed.), pp. 179 – 205, Cambridge, MA: MIT Press, 1993.

[7] D. J. Heeger and P. C. Teo, "A model of perceptual image fidelity," *Proc. of IEEE Int'l Conf. on Image Proc.*, Oct. 23 – 26 1995, Washington, D.C., USA, pp. 343 – 345.

[8] P. C. Teo and D. J. Heeger, "Perceptual image distortion," vol. SPIE 2179, 1994, pp. 127 – 141.

[9] S. J. P. Westen, R. L. Lagendijk, and J. Biemond, "Perceptual image quality based on a multiple channel HVS model," *Proc. of IEEE Int'l Conf. on Acoust., Speech and Sig. Proc.*, 1995, pp. 2351 – 2354.

[10] A. B. Watson, "The cortex transform: Rapid computation of simulated neural images," *Comput. Vision Graphics and Image Process.*, vol. 39, no. 3, pp. 311 – 327, September 1987.

[11] S. Comes, O. Bruyndonckx, and B. Macq, "Image quality criterion based on the cancellation of the masked noise," *Proc. of IEEE Int'l Conf. on Acoust., Speech and Sig. Proc.*, 1995, pp. 2635 – 2638.

[12] D. G. Hubel and T. N. Wiesel, "Receptive fields, binocular interaction, and functional architecture in the cat's visual cortex," *Journal of Physiology (London)*, vol. 160, pp. 106 – 154, 1962.

[13] F. W. Campbell and J. G. Robson, "Application of Fourier analysis to the visibility of gratings," *Journal of Physiology (London)*, vol. 197, pp. 551 – 566, 1968.

[14] L. Maffei and A. Fiorentini, "The visual cortex as a spatial frequency analyzer," *Vision Research*, vol. 13, pp. 1255 – 1267, 1973.

[15] S. Marčelja, "Mathematical description of the responses of simple cortical cells," *J. Opt. Soc. Am.*, vol. 70, no. 11, pp. 1297 – 1300, 1980.

[16] D. Gabor, "Theory of communication," *J. Instn Elect Engrs*, vol. 93, no. 26, pp. 429 – 459, 1946.

[17] J. G. Daugman, "Uncertainty relation for resolution in space, spatial frequency, and orientation optimized by two-dimensional visual cortical filters," *J. Opt. Soc. Am. A*, vol. 2, no. 7, pp. 1160 – 1169, 1985.

[18] J. P. Jones and L. A. Palmer, "An evaluation of the two-dimensional Gabor filter model of simple receptive fields in the cat striate cortex," *Journal of Neurophysiology*, vol. 58, no. 6, pp. 1233 – 1258, 1987.

[19] M. A. Webster and R. L. De Valois, "Relationship between spatial-frequency and orientation tuning of striate-cortex cells," *J. Opt. Soc. Am. A*, vol. 2, no. 7, pp. 1124 – 1132, 1985.

[20] R. L. De Valois, D. G. Albrecht, and L. G. Thorell, "Cortical cells: bar and edge detectors, or spatial frequency filters," in *Frontiers in Visual Science* (S. J. Cool and E. L. Smith, III, eds.), NY, NY: Springer-Verlag, 1978.

[21] J. J. Kulikowski and P. O. Bishop, "Fourier analysis and spatial representation in the visual cortex," *Experientia*, vol. 37, pp. 160 – 163, 1981.

[22] D. A. Pollen and S. F. Ronner, "Phase relationships between adjacent simple cells in the visual cortex," *Science*, vol. 212, pp. 1409 – 1411, 1981.

[23] T. S. Lee, "A bayesian framework for understanding texture segmentation in the primary visual cortex," *Vision Research*, vol. 35, no. 18, pp. 2643 – 2657, 1995.

[24] A. K. Jain and F. Farrokhnia, "Unsupervised texture segmentation using Gabor filters," *Pattern Recognition*, vol. 24, no. 12, pp. 1167 – 1186, 1991.

[25] D. F. Dunn and W. E. Higgins, "Optimal Gabor filters for texture segmentation," *IEEE Trans. on Image Processing*, vol. 4, no. 7, pp. 947 – 964, July 1995.

[26] T. N. Tan, "Texture edge detection by modelling visual cortical channels," *Pattern Recognition*, vol. 28, no. 9, pp. 1283 – 1298, September 1995.

[27] R. Navarro and J. Portilla, "Robust method for texture synthesis-by-analysis based on a multiscale Gabor scheme," *Human Vision and Electronic Imaging*, vol. SPIE 2657, Jan. 29 – Feb. 1 1996, San Jose, CA, USA, pp. 86 – 97.

[28] D. J. Heeger and J. R. Bergen, "Pyramid-based texture analysis/synthesis," *Proc. of IEEE Int'l Conf. on Image Proc.*, vol. 3, Oct. 23 – 26 1995, Washington, D.C., USA, pp. 648 – 650.

[29] G. Naghdy, J. Wang, and P. Ogundona, "Texture analysis using gabor wavelets," *Human Vision and Electronic Imaging*, vol. SPIE 2657, Jan. 29 – Feb. 1 1996, San Jose, CA, USA, pp. 74 – 85.

[30] M. W. Cannon, "Model of mechanisms mediating spatial pattern perception," *Proc. of the Human Factors Society 36th Annual Meeting*, 1992, Santa Monica, CA, USA, pp. 1430 – 1434.

[31] J. Yang and W. Makous, "Modeling pedestal experiments with amplitude instead of contrast," *Vision Research*, vol. 35, no. 14, pp. 1979 – 1989, 1995.

[32] J. Nachmias and R. V. Sansbury, "Letter to the editors, Grating contrast: Discrimination may be better than detection," *Vision Research*, vol. 14, pp. 1039 – 1042, 1974.

[33] F. W. Campbell and J. J. Kulikowski, "Orientational selectivity of the human visual system," *Journal of Physiology (London)*, vol. 187, pp. 437 – 445, 1966.

[34] M. R. Scheessele, S. M. Graham, and Z. Pizlo, "The exponential pyramid as a model of the human visual system," *Proc. of the Image and Multidimensional Signal Proc. Workshop*, 1996, pp. 108 – 109.

[35] Z. Pizlo, M. Salach-Golyska, and A. Rosenfeld, "Curve detection in a noisy image," *Vision Research*, vol. in press.

[36] J.-M. Jolion and A. Rosenfeld, *A pyramid framework for early vision*. Dordrecht: Kluwer Academic Pub., 1994.

[37] A. Rosenfeld, "Pyramid algorithms for perceptual organization, Special Issue: Computers in vision research," *Behavior Research Methods, Instruments, and Computers*, vol. 18, no. 6, pp. 595 – 600, 1986.

[38] T. S. Lee, "Image representation using 2D Gabor-wavelets," *IEEE Trans. on Pattern Analysis and Machine Intelligence*, vol. 18, no. 10, pp. 959 – 971, October 1996.

[39] F. W. Campbell, G. F. Cooper, and C. Enroth-Cugell, "The spatial selectivity of the visual cells of the cat," *Journal of Physiology (London)*, vol. 203, pp. 163 – 176, 1969.

[40] J. G. Daugman, "Quadrature-phase simple-cell pairs are appropriately described in complex analytic form," *JOSA Communications*, vol. 10, no. 7, pp. 375 – 377, 1993.

[41] R. L. De Valois, D. G. Albrecht, and L. G. Thorell, "Spatial frequency selectivity of cells in macaque visual cortex," *Vision Research*, vol. 22, pp. 545 – 559, 1982.

[42] D. A. Pollen and S. F. Ronner, "Visual cortical neurons as localized spatial frequency filters," *IEEE Trans. on Systems Man and Cybernetics*, vol. 13, no. 5, pp. 907 – 916, 1983.

[43] P. H. Schiller, B. L. Finlay, and S. F. Volman, "Quantitative studies of single-cell properties in monkey striate cortex. II. Orientation specificity and ocular dominance," *Journal of Neurophysiology*, vol. 39, no. 6, pp. 1320 – 1333, 1976.

[44] D. G. Stork and H. R. Wilson, "Do Gabor functions provide appropriate descriptions of visual cortical receptive fields?," *J. Opt. Soc. Am. A*, vol. 7, no. 8, pp. 1362 – 1373, 1990.

[45] J. A. Movshon, I. D. Thompson, and D. J. Tolhurst, "Spatial summation in the receptive fields of simple cells in the cat's striate cortex," *Journal of Physiology (London)*, vol. 283, pp. 53 – 77, 1978.

[46] R. L. De Valois and K. K. De Valois, *Spatial Vision*. New York, NY: Oxford University Press, 1988.

[47] M. S. Banks, W. S. Geisler, and P. J. Bennett, "The physical limits of grating visibility," *Vision Research*, vol. 27, no. 11, pp. 1915 – 1924, 1987.

[48] J. J. DePalma and E. M. Lowry, "Sine-wave response of the visual system. II. Sine-wave and square-wave contrast sensitivity," *J. Opt. Soc. Am.*, vol. 52, no. 3, pp. 328 – 335, 1962.

[49] H. A. Schober and R. Hilz, "Contrast sensitivity of the human eye for square-wave gratings," *J. Opt. Soc. Am.*, vol. 55, no. 9, pp. 1086 – 1091, 1965.

[50] F. L. Van Nes and M. A. Bouman, "Spatial modulation transfer in the human eye," *J. Opt. Soc. Am.*, vol. 57, no. 3, pp. 401 – 406, 1967.

[51] M. A. Losada, R. Navarro, and J. Santamaria, "Relative contributions of optical and neural limitations to human contrast sensitivity at different luminance levels," *Vision Research*, vol. 33, no. 16, pp. 2321 – 2336, 1993.

[52] E. Peli, R. B. Goldstein, G. M. Young, and L. E. Arend, Jr., "Contrast sensitivity functions for analysis and simulation of visual perception," *Digest of the Topical Meeting on Noninvasive Assessment of the Visual System*, 1990, Optical Society of America, Washington, DC, pp. 126 – 129.

[53] P. E. King-Smith and J. J. Kulikowski, "Pattern and flicker detection analyzed by subthreshold summation," *Journal of Physiology (London)*, vol. 249, pp. 56P – 57P, 1975.

[54] R. E. Fredericksen, P. J. Bex, and F. A. J. Verstraten, "How big is a Gabor patch, and why should we care," *J. Opt. Soc. Am. A*, vol. 14, no. 1, pp. 1 – 12, January 1997.

[55] D. J. Finney, *Probit analysis*. Cambridge Univ. Press, 3 ed., 1971.